Detection and Characterization of Striping in GOES-16 ABI VNIR/IR Bands

Haifeng Qian[a], Xiangqian Wu[b], Fangfang Yu[a], Xi Shao[a], Robert Iacovazzi[a], Zhipeng Wang[a] , Hyelim Yoo[a]

[a]ERT, Inc. Laurel, MD 20707 USA
[b]NOAA, NESDIS, STAR, College Park, MD 20740 USA

ABSTRACT

A new generation of imaging instruments, the Advanced Baseline Imager (ABI), was launched on November 19, 2016 aboard the first satellite of the Geostationary Operational Environmental Satellite – R Series (GOES-R). This premier satellite became GOES-16 shortly after launch, and replaced GOES-13 as NOAA's operational GOES-East satellite on December 18, 2017. ABI has 16 bands covering the spectrum between 0.47μm and 13.3 μm to provide continuous data stream for weather forecasting and disaster monitoring. After launch, it is critical to monitor and evaluate the instrument calibration performance in a timely manner using data processed by the GOES-16 Ground Segment, starting at Post-Launch Tests (PLT) and continuing throughout mission life. For this purpose, the GOES-16 Calibration Working Group (CWG) has developed an Instrument Performance Monitor (IPM) system that includes metrics for GOES-16 ABI striping identification and characterization. In particular, it includes individual band striping identification, flagging, frequency, and image quality provided at minute to mission-life time scales, and sample and pixel level. Using this tool, severe striping in several ABI bands – e.g., band01-03, band05, and band14-16 were characterized. The root cause of striping has been found to predominately arise from calibration algorithm deficiencies and artifacts. Identification and characterization of such striping thus motivates root-cause study and calibration improvement activities. Working as part of the CWG IPM system, the striping identification and characterization metrics help to make the user well informed of Ground Segment implemented calibration improvements and updates for GOES-16 ABI, but also provides clues for resolving anomalies.

Keywords: GOES-16 ABI, Radiometric Calibration, Striping, Identification and Characterization, Detector gain, Quadratic coefficients.

1. INTRODUCTION

The GOES-16, was launched on November 19, 2016. The primary instrument Advanced Baseline Imager (ABI) aboard is a new generation of imaging instruments providing three times more spectral information, four times the spatial resolution, and more than five times faster coverage than the legacy GOES system (Schmit et al. 2005; Kalluriet et al. 2018). It plays a critical role in supporting the advanced imagery and atmospheric measurements of Earth's weather, oceans and environment. ABI views the Earth with 16 different spectral bands (compared to five on the previous generation of GOES), including two visible channels, four near-infrared channels, and ten infrared channels, covering the spectrum between 0.47μm and 13.3μm (Table 1). ABI Level-1b (L1b) nominal sub satellite **s**patial resolution for visible band02 (0.64 μm) is 0.5km, 1.0km for band01, 03, 05 and 2.0km for all other bands. The default mode timeline 3 concurrently takes a full disk image every 15 minutes, an image of the continental U.S. every five minutes, and two smaller, more detailed images of areas where storm activity is present, every 60 seconds. The ABI can also operate in continuous full disk mode, providing uninterrupted scans of the full disk every 5 minutes in timeline 4. ABI infrared (IR) bands have on-orbit calibration within a single timeline, while visible-near-infrared (VNIR) bands use solar calibration.

After GOES-16 launch, it is critical to monitor and evaluate the instrument calibration performance in a timely manner using data processed by the GOES-16 Ground Segment (GS), starting at Post-Launch Tests (PLT) and continuing throughout mission life (Yu, et al. 2017; Kalluriet et al. 2018). For this purpose, the GOES-16 Calibration Working Group (CWG) has developed an Instrument Performance Monitor (IPM) system that includes

Earth Observing Systems XXIII, edited by James J. Butler, Xiaoxiong (Jack) Xiong, Xingfa Gu, Proc. of SPIE Vol. 10764, 107641N · © 2018 SPIE · CCC code: 0277-786X/18/$18 · doi: 10.1117/12.2321100

metrics for GOES-16 ABI striping identification and characterization. Satellite image striping is common phenomenon, in which individual detector appears brighter or darker than their neighboring detectors. In general, true striping, or "calibration striping", occurs during calibration processing and is caused by incorrect relative detector gains, which cause single detectors within the image to be brighter or darker than their neighbors, creating stripes along the scan. Imperfect calibration relates to instrumental design and calibration algorithm is the key cause, such as mirror side, gain stage, electronic unit, polarization, and stray light leaking. The striping noise needs to be quantified and corrected by reprocessing the data with accurate relative detector gains for the image analysis and satellite products (Cao et al. 2012; Liu et al. 2013; Bouali et al. 2014). In this study, we introduced a simple and robust striping algorithm to identify and characterize the striping for the GOES-16 6 VNIR bands and 10 IR bands. The results will be provided since the availability of ABI L1b data from January of 2017.

Table 1. GOES-16 16 bands Focal Plan Mode (FPM) properties.

FPM	Band	Wavelength (μm)	Detectors	Detector Type	Resolution (km)
VNIR	1	0.47	676	SiliconPINDiode	1
	2	0.64	1460	SiliconPINDiode	0.5
	3	0.86	676	SiliconPINDiode	1
	4	1.38	372	HgCdTe HDVIP	2
	5	1.61	676	HgCdTe HDVIP	1
	6	2.25	372	HgCdTe HDVIP	2
MWIR	7	3.9	332	HgCdTe HDVIP	2
	8	6.18	332	HgCdTe HDVIP	2
	9	6.95	332	HgCdTe HDVIP	2
	10	7.34	332	HgCdTe HDVIP	2
	11	8.5	332	HgCdTe HDVIP	2
LWIR	12	9.61	332	HgCdTe HDVIP	2
	13	10.35	408	HgCdTe MBE DLPH	2
	14	11.2	408	HgCdTe MBE DLPH	2
	15	12.3	408	HgCdTe MBE DLPH	2
	16	13.3	408	HgCdTe MBE DLPH	2

2. METHODOLOGY AND DATA

In this study, GOES-16 ABI striping proxy data is based on GOES-16 ABI L1b images. The ABI L1b radiance product is computed from Level 0 instrument detector samples that are resampled to pixels on the ABI fixed grid. The ABI fixed grid is a projection relative to the ideal location of a satellite in geostationary orbit. Each scene is comprised of one or more straight line scans called “swaths”. The Full Disk scene includes twenty-two swaths, the CONUS scene is made up of six swaths, and a MESO scene incorporates two swaths. The swaths from different scenes are generally interleaved in a timeline when scanning multiple scenes. The CONUS scene coverage area is approximately 5000 km in the east-west direction by 3000 km in the north-south direction. The coverage area of a mesoscale scene is approximately 1000 km by 1000 km (Table 2).

Table 2. GOES-16 ABI L1b timeline product data variable dimensions

Resolution		Full Disk		CONUS		Mesoscale	
km	micro-	N/S	E/W	N/S	E/W	N/S	E/W
(nadir)	radians	(y-axis)	(x-axis)	(y-axis)	(x-axis)	(y-axis)	(x-axis)
0.5	14	21696	21696	6000	10000	2000	2000
1	28	10848	10848	3000	5000	1000	1000
2	56	5424	5424	1500	2500	500	500

Image-by-Image scanning for striping identification is expensive in computation and impractical for a real-time purpose, especially for full disk and CONUS mode. It is also limited to the nature of quick evolution of large scale atmosphere. Considering the fact that a striping is mostly due to imperfect calibration, its pattern normally appears

to be repeatable in the full disk/CONUS/MESO simultaneously, we thus used the MESO1 as the proxy for the real-time striping identification and trending. The L1b MESO1 dataset fixed gridded image array is 500x500 in low resolution bands, up to 2000x2000 in band02. When being processed, it significantly reduces the memory resource requirement for the computation, compared to the full disk mode. Similar procedure can be applied to CONUS, but only as the offline investigation. The selection of MESO1 in our study, rather than MESO2, is because MESO1 is usually used to trace the hurricane storm, which provides the perfect scenario to eyeball the striping pattern (if there is) in high reflective deep convertible hurricane clouds. Additionally, since the striping is due to the imperfect calibration and it normally lasts for a certain period (up to months) over the detectors or persists until being fixed, in practice we implemented an algorithm with hourly step averaging image, rather than minute step. This significantly reduces the computation and monitoring workforce, but keeps the striping features well. An offline package of minute image-by-image scanning for striping is also ready to serve for dive-in investigation.

The simple and robust algorithm of striping identification is briefed as shown in Figure 1 and following equations. A variable BT(x, y, t) is designed as the brightness temperature of IR (same for reflectance in VNIR bands), which varies in longitude, latitude and time dimensions. Striping identification procedure follows the steps:

1) Mean on X, 1-hour T dimensions $BTxt(Y)$

$$BTxt(Y) = \overline{\sum_{xt} BT(x,y,t)} \quad (1)$$

2) 11-point smoothing function on Y dimension:

$$sBTxt(Y) = f(BTxt(Y)) \quad (2)$$

3) Calculate the anomaly by de-trending:

$$BTxt\_dtr(Y) = BTxt(Y) - sBTxt(Y) \quad (3)$$

4) Neighboring difference for dBTxt(Y) in Y dimension to enhance the signal:

$$dBTxt(Y)_n = BTxt\_dtr(Y)_{n+1} - BTxt\_dtr(Y)_n \quad (4)$$

5) Calculate the striping index with the threshold:

$$Stripe\_idx(Y) = f(dBTxt(Y), threshold) \quad (5)$$

In processing, each time we scan 60 MESO1 images in an hour and calculate the striping index (Figure 1b). The striping is expressed as an index which is latitude-dependent. This hourly index will be saved into an index matrix over time. In particular, it includes individual band striping identification, flagging, frequency, and image quality information provided at minute to mission-life time scales, and sample and pixel-level spatial scales. With this matrix, a statistical analysis can provide from a daily routine to life-time the status of the instrument performance and calibration improvement monitoring. As we point out, the striping sometimes is very subtle and masked by the background environment, not easily seen by eye. Since the index is dependent on thresholds, this algorithm with our threshold is not guaranteed to identify all the striping, but the results have proved its capability to identify and characterize the major striping of our interests for calibration purpose.

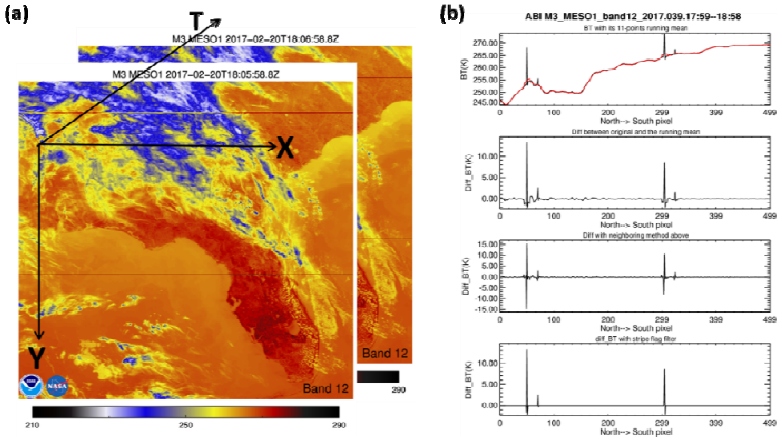

Figure 1. (a) A typical striping example of IR band12 L1b brightness temperature (BT) with the dimension in X, Y, T. The time dimension is 1-minute-step MESO1 image. Similar for the reflectance of VNIR bands. (b) An example of step-by-step striping identification for band12 following the equations 1 to 5. The bottom image shows the BT anomaly only at the striping lines.

3. ANALYSIS AND RESULTS

With the hour-bin striping index matrix, we conduct a serious of statistical analysis, including individual band striping identification, flagging, frequency, and image quality information. In this section, we separate our analysis and results into two parts: VNIR bands and IR bands. For each part, an overall performance of each bands since GOES-16 launch will be presented firstly, then temporal and spatial features of striping in the individual band will be characterized. The root cause or the correction algorithm will be discussed based on our calibration knowledge in these bands. In this study, the selected band01-02 striping reduction due to the new Look-Up-Table (LUT) and the new scheme will be discussed in the VNIR bands section. The selected Band014 striping reduction will be briefly presented in the IR bands section.

3.1 VNIR Bands striping

Figure 2 presents overall VNIR bands status in two different perspectives. Figure 2a is overall striping occurrence possibility in percentage for ABI VNIR bands, mostly in term of temporal scale. It conveys to what degree the striping have been occurred in the VNIR bands. In practice, value of 1 is assigned to the hour when the string occurs in striping index matrix, and 0 is for the hour without striping identified. Striping occurrence possibility then was calculated by averaging those values. This index helps to inform overall of the striping occurrence since its launch. It shows that band01/02/05 are the bands with larger occurrence 20%, compared to 10% in band03 and band06. Band04 is a safe band with very less occurrence, relatively. It is notable that since VNIR bands doesn't have a light at night, if the night images were excluded, the percentage will be doubled. To study the image striping lines frequency, we also calculated overall occurrence ratio on striping lines in percentage for VNIR bands (Figure 2b). Contrast to Figure 2a, Figure 2b conveys the information of spatial scale. It calculates the ratio of striping line to the total image lines. Clearly, band01/02 registered more lines of striping than band05, although both of them has the similar possibility as band05 (Figure 2a). For example of band02, nearly 1.5% of total 2000 lines, roughly 60 lines (after day-night adjustment) were identified the striping, which for band05, only 4 lines of image shows the striping. Band03/06 shows few lines of striping overall and band04 is nearly clear. In the following part, we will explore deeply the striping temporal and spatial pattern for band01/02. We also provide our investigation of root causes with the tools, such as CWG IPM and GRATDAT, a software to unpack GOES-16 ABI L0 dataset to L1a (uncalibrated). We injected ABI L1a from GRATDAT with the designed gain into our in-house VNIR bands calibration package to convert L1a to L1alpha image (calibrated radiance but not navigated). The L1alpha can server as a proxy for evaluate the calibration performance.

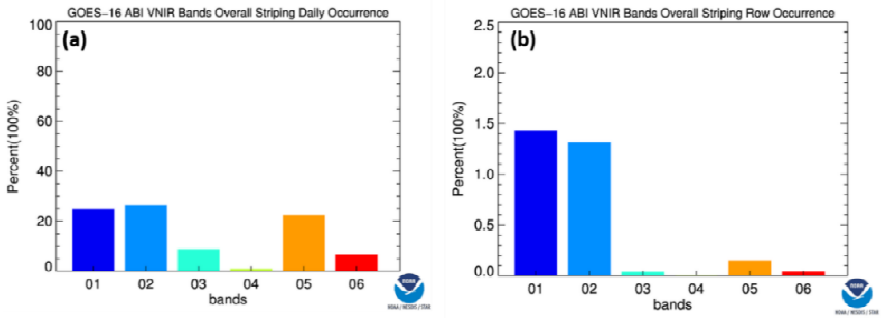

Figure 2: (a) Statistical analysis of overall striping occurrence possibility in percentage for ABI VNIR bands. (b) Overall ratio of striping occurrence to total ABI image lines in percentage for ABI VNIR bands.

3.1.1 Striping in ABI Band01-band02

ABI VNIR band01/02 have suffered striping since the GOES-16 launch. Figure 3a shows the daily striping occurrence for each VNIR bands. The daily striping occurrence is calculated with the hour-bin of striping index. Figure 3b shows the daily striping lines occurrence ratio for each VNIR bands. It is clear that before 02/07/2018, ratio of lines with striping in band01/02 was significantly higher than the later time in Figure 3b. This striping reduction is due to a new algorithm implemented in the Ground Segment (GS) system. In this new algorithm, a new quadratic coefficients Q-LUT for band1 (0.47µm), band 2 (0.64 µm), band3 (0.86µm) is used. The below Eq6 is the

new gain calibration equation and Eq7 is for earth radiance calibration. Additionally, a quadratic scaling (Q-scaling) scheme in all VNIR bands was used when calculating the VNIR bands gain, compared to previous one without $f_{int,ch}$ in the Q part.

$$m = \frac{f_{int,ch} \cdot L_{SCT}^{eff}}{(\bar{x}_{SCT} - \bar{x}_{Solar\_Cal\_Space})} - Q \frac{(\bar{x}_{SCT} - \bar{x}_{Solar\_Cal\_Space})}{f_{int,ch}} \quad (6)$$

$$Rad = m * DN + Q * DN * DN \quad (7)$$

Where m denotes VNIR band gain, $f_{int,ch}$as Solar calibration Integration factor 9, L_{SCT}^{eff} as Effective ICT channel average spectral radiance, and Q is Quadratic coefficient for each detector in bands. $\bar{X}$ is the average of scene count for solar calibration and space look view, reprehensively. The on-orbit measurement follows the calibration equation (Eq7) to convert the scene count into radiance. Rad is for the calibrated Earth radiance. DN is for delta count from the raw Earth count with subtracting the background space look view count.

Though the new Q value magnitude from LUT is larger (not shown here) than the previous one before 02.07.2018, $f_{int,ch}$has the value of 9 and brings the new Q-scaling to suppress the impact of the nonlinear contribution in gain calculation. After the new Q LUT and Q-scaling scheme were implement in Operational Environment (OE) on 02.07.2018, the striping in band01/02 were significantly reduced as shown in the Figure 4. However, we do see the striping occurrence up to 30% in Figure 3a, which implies that there is a residual striping registering in some detectors in the band01/02, but less lines and much subtle. Note that the residual subtle striping is very subtle, not easily to be seen by eyes. The characterization of these residual striping and further possible calibration improvement is beyond this study currently.

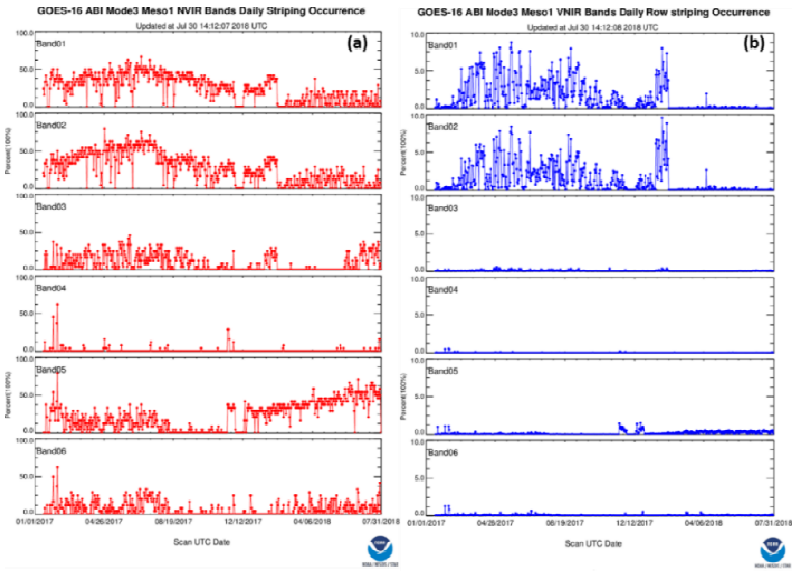

Figure 3. (a) Statistical analysis of striping occurrence possibility in percentage for individual VNIR bands since 2017. (b) Ratio of striping occurrence to total ABI image lines in percentage for ABI VNIR bands.

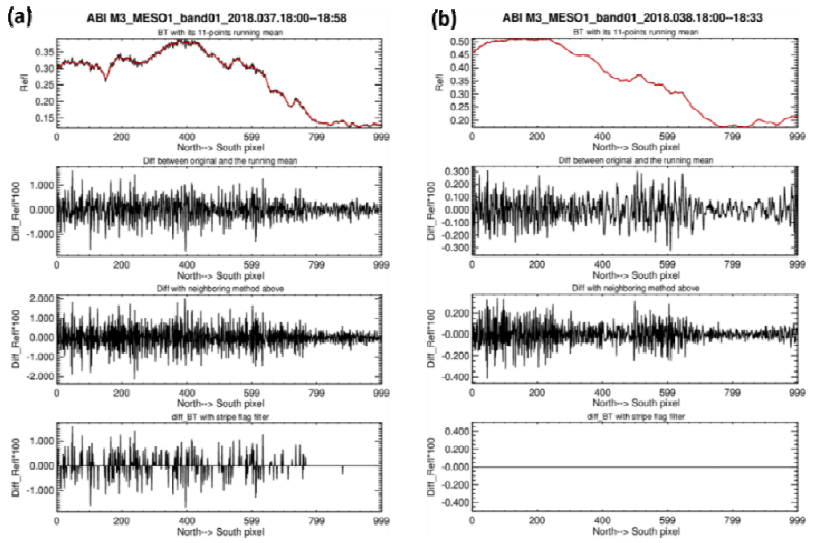

Figure 4. (a) Step-by-step striping identification for band01 with the L1b MESO1 18:00-18:59UTC on 02.06.2018 before the new Q-LUT and Q-scaling scheme implemented. (b) Same as (a) but with MESO1 18:00-18:59UTC on 02.07.2018 after the new algorithm implemented. Significant striping reduction were observed.

3.2 IR Bands Striping

Figure 5 presents the views of overall striping status for all GOES-16 ABI IR bands (band07-band16) since January, 2017. Figure 5a is overall striping occurrence possibility in percentage, reflecting their temporal variation. Different from the fact that VNIR bands don't have light at night time, IR bands can be conducted with L1b image striping scanning for daily 24 hours. The Figure 6a shows that band14/16 are the bands with larger occurrence over 70% in life time till recently, compared to less than 20% in band07,10,11,12,13,15. Band08/09 are a safe band with less occurrence both in the temporal and spatial scale. Considering that IR band07-16 MESO1 image has a dimension of 500x500, Band14 was registered more lines of striping than other bands. 0.5% (approximately 2.5) lines of image shows the striping since 2017 in averaging. Band07/12/16 has about 1 line showing striping overall. Figure 6 shows the striping pattern evolution in daily timing for individual IR bands. Generally, band14/16 have suffered with the striping seriously and consistently since 2017(Figure 6). Band08/09 has not been with striping for most of time. A period of 100% were found in both band10 and 12. For band7, band11 and band13, striping was also found. In the following part, we will focus on the striping temporal and spatial pattern for 14-16 of our interests. The detailed root cause of striping is briefed here and the detailed discussed can be found in the report about the IR image quality assessment from STAR-CWG group (Wang et al 2018).

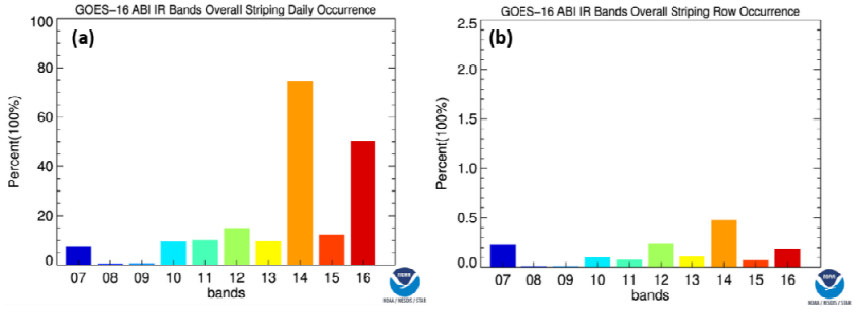

Figure 5 (a) Statistical analysis of overall striping occurrence possibility in percentage for ABI IR bands. (b) Overall ratio of striping occurrence to total ABI image lines in percentage for ABI IR bands.

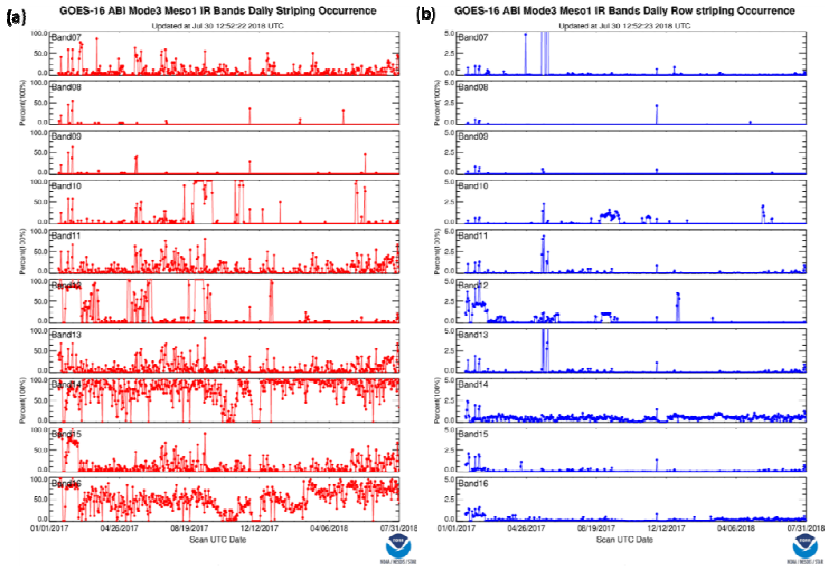

Figure 6 Statistical analysis of striping occurrence possibility in percentage for individual IR bands since 2017. (b) Ratio of striping occurrence over the ABI image lines in percentage for individual IR bands.

ABI band14 (11.2μm) is one of the most important band for GOES-16 L2 products. It is the traditional longwave infrared window band enables operational meteorologists to diagnose discrete clouds and organized features for general weather forecasting, analysis, and broadcasting applications. The striping in this band thus will impact the accuracy of those products. The striping was consistent in position of L1b image since GOES-16 launch (Figure 7). STAR-CWG IR bands scientist conducted the investigation and found that the striping lines were related to the calibration nonlinearity, which is due to very large negative Q values. As shown in the Figure 8a, for band14, only 6 of 408 detectors have non-zero negative values. Among them, the three detectors (#176/250/307) with large negative Q values not only produced large positive gain in the detector, but also extremely enlarged the calibration nonlinear contribution, leading to lower radiance (striping), comparing to the neighboring. Such kind of phenomenon also occurred in band15 on the detector 231 and band16 on the detector 221 (Figure 8a). After identification of this root cause, a sensitivity calibration testing with zero Q values at those detectors were carried out and was successful in removing the striping(Wang et al. 2018). CWG and GS are working to implement the new Q value LUTs for band14-16.

A double strong striping lines (up to 4K anomaly in BT compared to the neighboring) were found in the band10 MESO1 image during the period of 05.01.2017 to 10.03.2017, which was caused by Band10 detector 312 failure and was removed with the Best-Detector-Select (BDS) update on 10.03.2017. Also on band12, a strong striping was observed since January of 2017, which was caused by the failure of band12 detector 257 and was removed with the BDS update on 10.03.2017. And furthermore, a short period of striping during 12.30.2017 to 01.02.2018 was detected for at band12 detector 290 and 291 and the corresponding stripes were removed with the BDS update on 01.02.2018. Another striping period of 02.06.2018 to 03.05.2018 was found due to the band12 detector 309 and was removed with the BDS update on 03/05/2018.

CWG also did found a short period of striping for other IR bands. For example, the striping was observed in the striping-clear band08 (6.18μm) L1b image, starting from 00:21:00Z on 04.29.2018. This is caused by the space look digital count latch-up of detector 87 phenomenon, which has occurred to other bands/detectors previously. This detector failure was recovered quickly by GS. For band7, band11 and band13, striping were found and the root cause investigation is been conducted by CWG IR band scientists.

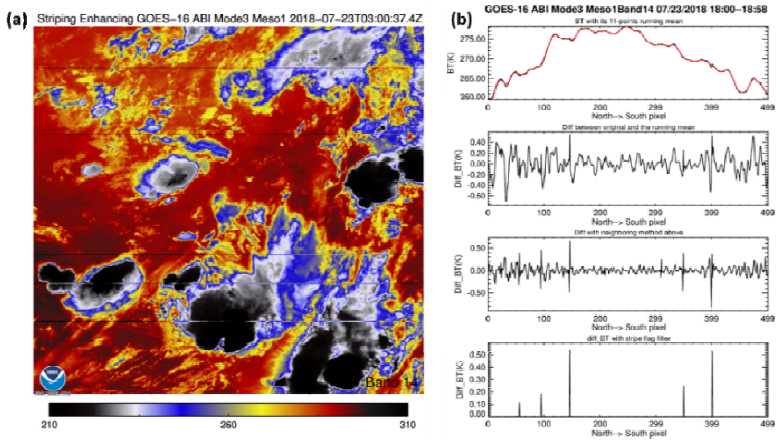

Figure 7. (a) Example of band14 L1b image with "enhanced" striping. (b) Striping identification for band14 following the equation xxx.

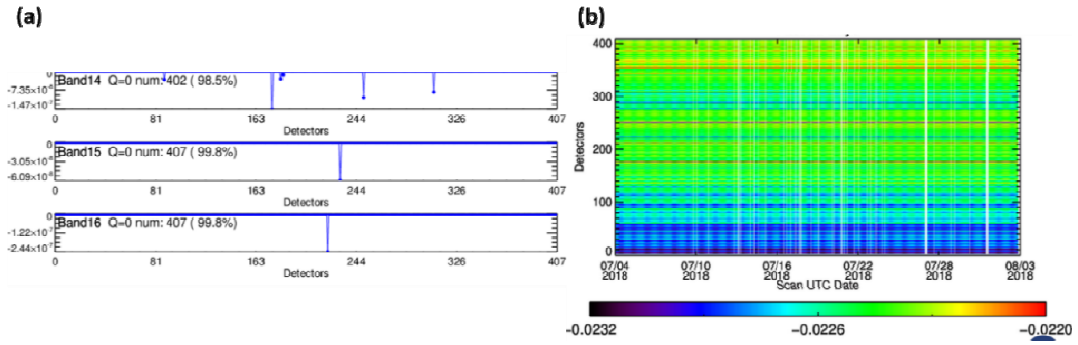

Figure 8. (a) Q values of BDS for band14-16 from CDRL79 Version H. (b) Band14 on orbit detector gain from 07.03.2018 to 08.03.2018. The detectors with large negative Q values normally have large positive anomaly gain compared to the neighboring.

4. SUMMARY AND DISCUSSION

Since the launch of GOES-16 ABI on November 19, 2016, it is critical to monitor and evaluate the instrument calibration performance. In this study, besides of CWG Instrument Performance Monitor (IPM) system, a simple and robust striping identification algorithm was developed to identify and characterize the striping with the proxy from the 6 VNIR and 10 IR bands of GOES-16 ABI L1b MESO1 images. With this tool, band-dependent striping was successfully identified and characterized in the temporal and spatial scale. The root cause of the striping has been found to predominately arise from calibration algorithm deficiencies and artifacts in selected band01-02, band03, band05 and IR band14-16. In band01-03, a new Q-LUT and Q scaling schemed was implemented in the ground system on 02.07.2018 and significantly reduced the striping. As one of most important IR bands, band14 striping was attributed to the large negative Q values in several detectors. Striping in band10 and band12 associated with the detector failure was removed with GS BDS updates on those detectors. In general, this striping metrics have motivated important root-cause study and calibration improvement activities. It not only helps to make the user well informed of GS implemented calibration improvements and updates for GOES-16 ABI, but also provides clues for resolving anomalies. Part of the underlying root cause are still under investigation.

5. ACKNOWLEDGEMENT

The authors thank to GOES-R Calibration Working Group (CWG)/NOAA, flight groups, and the ABI instrument vendor. We are also grateful to NOAA anonymous reviewers for helpful comments and discussions to

the manuscript. This work is funded by GOES-R program. The manuscript contents are solely the opinions of the authors and do not constitute a statement of policy, decision, or position on behalf of NOAA or the U.S. government.

REFERENCES

[1] Schmit, T. J., Gunshor, M.M., Paul, W., Menzel, Gurka, J., Li, J. and Bachmeier J., "Introducing the next-generation advanced baseline imager (ABI) on GOES-16", Bull. Am. Meteorol. Soc., 86, 1079– 1096, doi:10.1175/BAMS-86-8-1079 (2005).

[2] Kalluriet, S., Alcala, C., Carr, J., Griffith, P., Lebair, W., Lindsey, D., Race, R., Wu, X. Q. and Zierk, S., "From photons to pixels: processing data from the advanced baseline imager," Remote Sens.10, 177 (2018). https://doi.org/10.3390/rs10020177

[3] Cao, Y.T., Yan, D. M., Wang, G. and You, S., "De-striping algorithm in ALOS satellite imagery based on adaptive frequency filter. Image and Signal Processing for Remote Sensing XVIII,L. Bruzzone, Ed., International Society for Optical Engineering (SPIE Proceedings, Vol. 8537), 853719, doi:10.1117/12.973674 (2012).

[4] Liu, Q. H., Cao, C. Y. and Weng, F. Z., "Striping in the Suomi NPP VIIRS thermal bands through anisotropic surface reflection" J. Atmos. Ocean. Technol. vol. 30 pp. 2478-2487 (2013).

[5] Bouali, M. and Ignatov, A., "Adaptive reduction of striping for improved sea surface temperature imagery from Suomi National Polar-Orbiting Partnership (S-NPP) Visible Infrared Imaging Radiometer Suite (VIIRS)" J. Atmos. Ocean. Technol. vol. 31 pp. 150-163 (2014).

[6] Yu, F. F., Wu, X. Q., Shao, X., Efremova, B.V., Yoo, H., Qian, H. and Iacovazzi, R.A., "Early radiometric calibration performances of GOES-16 Advanced Baseline Imager (ABI)". Proc. SPIE **2017**, *10402*, 104020S (2017).

[7] NOAA GOES-16 Series ABI Beta, Provisional and Full Validation Readiness, Implementation and Management Plan (RIMP), 416-R-RIMP-0315, Version 1.1, July 2016

[8] Product Definition and Users' Guide (PUG), Vol 3: LeveL1b Products for GOES-16 Series Core Ground Segment, Harris Corporation, Revision D, May (2015).

[9] Wang Z. et al. GOES-16 Calibration Working Group report, College Park, Maryland, June (2018)

[10] CDRL0079_PFM-VOL1_REVH_ABI_Calibration_Handbook: Calibration Data Books, CDRL No. 0079_PFM-Vol1_Rev-H, Groundstation Processing Inputs (2017-11-07)

[11] CDRL0080-3F_ABI_GPA_Calibration: Ground Processing Algorithm Description: Calibration CDRL No. 80-3F.